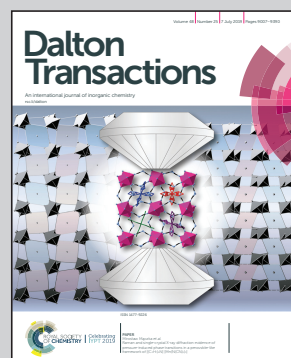


Showcasing unexpected tin redox chemistry as observed by Dr. Lundberg and Prof. Persson at the Department of Molecular Sciences, Swedish University of Agricultural Sciences, Uppsala.

On solvated tin(IV) ions and the coordination chemistry of high-valent d¹⁰ metal ions

During a slow redox reaction in dimethylsulfoxide at room temperature part of the solvent is reduced and tin(II) oxidized to tin(IV) while forming a Sn–C bond, without any catalysts or other reactants.

As featured in:



See Daniel Lundberg and Ingmar Persson, *Dalton Trans.*, 2019, **48**, 9089.



ROYAL SOCIETY
OF CHEMISTRY | Celebrating
IYPT 2019

rsc.li/dalton

Registered charity number: 207890



Cite this: *Dalton Trans.*, 2019, **48**, 9089

Received 13th March 2019,
Accepted 29th April 2019

DOI: 10.1039/c9dt01097a

rsc.li/dalton

On solvated tin(IV) ions and the coordination chemistry of high-valent d¹⁰ metal ions†

Daniel Lundberg * and Ingmar Persson

A very slow oxidation of dimethylsulfoxide (dmso) solvated tin(II) ions in solution results in the formation of a crystalline, structurally determined compound, $[\text{CH}_3\text{Sn}(\text{OS}(\text{CH}_3)_2)_5](\text{ClO}_4)_3$, whereas a similar reaction in *N,N*-dimethylthioformamide (dmft) forms a crystalline solid with a proposed binuclear $[\text{Sn}_2(\text{SH})_2(\text{SCH}(\text{CH}_3)_2)_8]^{6+}$ entity but whose exact formula remains undetermined. Both solids precipitate with time in their respective mother liquids and constitute the first two tin(IV) and even tetravalent d¹⁰ metal ion solvate complexes ever reported. An EXAFS study showed that the structure of the $[\text{CH}_3\text{Sn}(\text{OS}(\text{CH}_3)_2)_5]^{3+}$ complex is identical in solid state and dmso solution. While the exact chemical reaction pathways are unknown, the formation of these complexes constitute a novel way of obtaining solvated tin(IV) ions in standard, commonplace organic media.

Introduction

The current research of solar cells focuses heavily on different forms of perovskite structures as the light-harvesting active layer.¹ Very often, such structures include a lead or tin halide-based material, which has increased the efficiency drastically over the last few years using two main routes of manufacturing: solution-processing techniques and chemical vapor deposition.² Fundamentally, both of these techniques are based upon the understanding of the electronic nature of these elements. Chemically speaking, the heavier elements in group 14, tin and lead, mainly feature oxidation states +II and +IV with preference for +II for lead and +IV for tin. Tin displays stable chemistry for both oxidation states in water, while the chemistry of lead is dominated by lead(II) with lead(IV) compounds being strong oxidants in aqueous systems. The coordination chemistry of tin(II) and lead(II) is strongly affected by occupied anti-bonding orbitals causing large voids, so-called *gaps*, in their coordination spheres.^{3–6} This is not the case for the tetravalent ions, but for neither tin(IV) nor lead(IV), no hydrate or solvate structures have previously been reported. We have made several attempts to prepare aqueous solutions of hydrated tin(IV) ions in strongly acidic solution, but it always resulted in precipitation of solid tin(IV) oxide, SnO_2 .

Department of Molecular Sciences, Swedish University of Agricultural Sciences, P.O. Box 7015, SE-750 07 Uppsala, Sweden. E-mail: daniel.lundberg@slu.se

† Electronic supplementary information (ESI) available: Fits of the raw EXAFS data and their Fourier transforms, plots of unit cells of the reported crystal structures and their respective crystallographic information files (.cif), and the summary of previously reported high-valent d¹⁰ structures in the solid state. CCDC 1873377. For ESI and crystallographic data in CIF or other electronic format see DOI: 10.1039/c9dt01097a

The coordination chemistry of tin(IV) with (hydr)oxide ions is strongly dominated by a few different types of tin(IV) ions: (i) hexahydroxidostannate(IV) complexes, $[\text{Sn}(\text{OH})_6]^{2-}$, (ii) polymeric six-coordinate stannate(IV) with the composition $(\text{SnO}_3^{2-})_n$ or $(\text{SnO}_4^{4-})_n$, (iii) tin(IV) oxide, but also (iv) six-, seven-, and eight-coordinate tin(IV) complexes commonly with bi- or tridentate oxygen donor ligands.^{7,8} The mean Sn–O bond distance in the $[\text{Sn}(\text{OH})_6]^{2-}$ complexes is 2.049 Å, in the polymeric edge-shared octahedral chains 2.056 and 2.060 Å for $(\text{SnO}_3^{2-})_n$ and $(\text{SnO}_4^{4-})_n$, respectively, and in tin(IV) oxide, 2.052 Å. The mean Sn–O bond distance for all six-coordinate stannate(IV) complexes of type (i–iii) is 2.052 Å, Table S1,† including almost 100 separate structures. With the exception of the hexahydroxidostannate(IV) compounds, only one other, simple tin(IV) complex, a hexanitratostannate(IV), has been reported, with a mean Sn–O bond distance of 2.072 Å.⁹ Also, five compounds with isolated tetrahedral tetraoxostannate(IV) ions, $[\text{SnO}_4]^{4-}$, with a mean Sn–O bond distance of 1.957 Å, are found in the literature, Table S1,†

The coordination chemistry of tin(IV) with various anionic organic O-donor ligands is also predominately six-coordinate, with a mean Sn–O bond distance of 2.054 Å, though a few seven- and eight-coordinate compounds have been reported with mean Sn–O bond distances of 2.127 and 2.175 Å, respectively, Table S1,† There are two examples of tin(IV) ions with a lower coordination number, both including *t*-butoxide: a four-coordinate compound with a mean Sn–O bond distance of 1.948 Å,¹⁰ and a five-coordinate one with mean Sn–O bond distance of 2.011 Å.¹¹

Not surprisingly, in tin(IV) complexes and compounds with sulfur-donor ligands, lower coordination numbers are more frequent than among oxygen donors, given the relatively larger



size and higher covalence of sulfur. The Cambridge Structural Database lists over 130 four-coordinate, 39 five-coordinate, and 45 six-coordinate tin(IV) structures with *S*-donors,⁸ and in addition a small number of binuclear complexes, Table S2.† Furthermore, a fairly large number of octahedral hexahalostannate(IV) complexes, particularly $[\text{SnF}_6]^{2-}$ and $[\text{SnCl}_6]^{2-}$, has been reported in the solid state,^{7,8} though they lie outside the scope of this structural investigation.

The aim of this study was to explore the contents of dimethylsulfoxide (dmso) and *N,N*-dimethylthioformamide (dmtf) solutions of tin(II) prepared for the study the coordination chemistry of tin(II).³ They were stored for 12 years in closed vessels at room temperature and, when opened, the dmso solution had an intense and characteristic smell of dimethylsulfide, $(\text{CH}_3)_2\text{S}$. This strongly indicated that at least part of the dmso had been reduced and that an oxidation product had formed. Similarly, in the dmtf solution, another oxidation product had formed, where tin(II) upon being oxidized to tin(IV) had reduced some of the dmtf.

Experimental section

Chemicals

The preparation procedures of the studied tin(II) dmso and dmtf solutions are described in detail elsewhere.³ These solutions were stored in closed glass vials at room temperature for 12 years. The volume of the dmso solution was reduced by evaporation under vacuum and pentakis(dmso)methyltin(IV) perchlorate, $[\text{CH}_3\text{Sn}(\text{OS}(\text{CH}_3)_2)_5](\text{ClO}_4)_3$, 1, precipitated after refrigeration. As for the dmtf solution, crystals had precipitated with time in the dmtf mother liquid, 2. However, the quality of these crystals was not sufficient for an accurate crystallographic structure determination, though it was possible to find the principle atomic arrangement.

Single-crystal X-ray diffraction

Data were collected on a Bruker SMART CCD 1 k diffractometer at ambient room temperature. The crystals were mounted in glass capillaries, which were sealed immediately after mounting. The structures were solved by standard direct methods in the SHELX 2016/6 program package¹² and refined by full matrix least-squares isotropically on F^2 and finally in anisotropic approximation on all non-hydrogen atoms, unless noted. Hydrogen atoms detected in the difference Fourier syntheses were added and refined using a riding model. All structure solutions were performed with the SHELXL 2016/6 programs in its PC version.¹² Selected crystal and experimental data is summarized in Table 1. Additional crystallographic data is available in Tables S3a and S3b.†

EXAFS data collection and treatment

X-ray absorption data was collected at the Stanford Synchrotron Radiation Lightsource (SSRL), using the unfocussed 8-pole wiggler beam line 4-1. SSRL operated at 3.0 GeV and a ring current of 200 mA in top-up mode. The radiation was mono-

Table 1 Crystallographic data and structure refinement details for compound 1, pentakis(dmso)methyltin(IV) perchlorate

	1
Formula	$[\text{CH}_3\text{Sn}(\text{dmso})_5](\text{ClO}_4)_3$
Sum formula	$\text{C}_{10}\text{H}_{31}\text{Cl}_3\text{O}_{18}\text{S}_5\text{Sn}$
M_w	824.71
Diffractometer system	Bruker Smart CCD
Radiation, $\lambda/\text{\AA}$	0.71073
Crystal system	Monoclinic
Space group	$P2_1/c$ (no. 14)
$a/\text{\AA}$	11.530(6)
$b/\text{\AA}$	15.232(8)
$c/\text{\AA}$	18.522(10)
$\alpha/^\circ$	90
$\beta/^\circ$	100.511(6)
$\gamma/^\circ$	90
$V/\text{\AA}^3$	3198(3)
T/K	296(2)
Z	4
$D_g/\text{g cm}^{-3}$	1.71
F^2	1664
μ/mm^{-1}	1.4
Crystal size/mm	0.4 × 0.3 × 0.2
θ range/°	2.60–25.68
Index ranges	$-13 \leq h \leq 14, -18 \leq k \leq 18, -22 \leq l \leq 22$
Measured reflections	25 122
Unique reflections	5179 ($R_{\text{int}} = 0.0233$)
Data/restraints/params	6057/173/386
Goodness of fit	1.037
Refinement method	Full-matrix least-sq. F^2
Final R_1 , wR_2 [$I > 2\sigma(I)$] ^a	0.0331, 0.0905
Final R_1 , wR_2 [all data]	0.0404, 0.0966
Max. peak/hole e \AA^{-3}	0.08/–0.52

^a *R* values are defined as: $R_1 = \sum ||F_{\text{o}}| - |F_{\text{c}}|| / \sum |F_{\text{o}}|$, $wR_2 = [\sum [w(F_{\text{o}}^2 - F_{\text{c}}^2)^2] / \sum [w(F_{\text{o}}^2)^2]]^{0.5}$; dmso = $\text{OS}(\text{CH}_3)_2$.

chromatized by a Si(220) double-crystal monochromator, which was detuned to 30% of maximum intensity to reduce higher order harmonics at the end the scans. The data was collected in transmission mode using ion chambers with a gentle flow of argon. Three scans per sample were collected and averaged.

The EXAFS oscillations were extracted from averaged raw data using standard procedures for pre-edge subtraction, spline removal and data normalization. In order to obtain quantitative information of the coordination structure of the tin(IV) complex, the experimental k^3 -weighted EXAFS oscillations were analyzed by linear least-squares fits of the data to the EXAFS equation, refining the model parameters number of backscattering atoms, N_i , mean interatomic distances R , Debye–Waller factor coefficients, σ^2 , and relative ionization energy, ΔE_{o} . Data analysis was performed using the EXAFSPAK program package.¹³ The energy scale of the X-ray absorption spectra was calibrated by assigning the first inflection point of a metallic tin foil to 29 198 eV.¹⁴ The sample cell for the solution was made of a 1.5 mm Teflon® spacer and 6 μm polypropylene X-ray film windows hold together with titanium frames. The solid was placed in a 2 mm thick aluminium frame with Mylar® tape windows. The analysis of the data was performed with the EXAFSPAK¹³ and FEFF7 program¹⁵ packages allowing the determination of the parameters of the local structure around the tin(IV) ion.





The standard deviations reported for the obtained refined parameters listed in Table 3 are those related to the least-squares refinements and do not include any systematic errors. Variations in the refined parameters obtained using different models and data ranges indicate that the accuracy of the distances given for the separate complexes is within ± 0.005 – 0.02 Å, which is typical for well-defined interactions.

Results and discussion

Structure of the dimethylsulfoxide solvated methyltin(IV) ion

Tin(II) is slowly oxidized to tin(IV) and dmso is reduced to dimethylsulfide, characterized by its intense smell, in a dmso solution of tin(II) perchlorate.³ After reducing the volume of the solution by evaporation and cooling in refrigerator crystals of pentakis(dmso)methyltin(IV) perchlorate $[\text{CH}_3\text{Sn}(\text{OS}(\text{CH}_3)_2)_5](\text{ClO}_4)_3$, **1**, of sufficient quality for a crystallographic study were obtained. The crystal structure of **1** shows that tin(IV) binds five dmso molecules, mean Sn–O bond distance 2.099 Å, and a methyl group at 2.113 Å in a slightly distorted octahedral fashion, with an overall mean Sn–O/C bond distance of 2.101 Å, Table 2. The methyl group originates from the deterioration products of reduced dmso, as tin(II) oxidizes to tin(IV), and the covalent Sn–C bond reduces the effective charge of the complex, thereby further stabilizing it. The structure of the $[\text{CH}_3\text{Sn}(\text{OS}(\text{CH}_3)_2)_5]^{3+}$ unit is shown in Fig. 1, selected Sn–O/C bond distances and O–Sn–O/C bond angles are given in Table 2, the position of the complex in the unit cell is shown in Fig. S1,[†] with the full .cif file listed in Table S3a.[†]

An EXAFS study of solid **1** and the dmso solution from which **1** precipitated show that the structure of the $[\text{CH}_3\text{Sn}(\text{OS}(\text{CH}_3)_2)_5]^{3+}$ unit is maintained in dmso solution as their EXAFS spectra can be superimposed on each other, Fig. 2, with structure parameters in very close agreement with the crystallographic structure of **1**.

Table 2 Selected bond lengths (in Ångström) and angles (in degrees) in **1**. Mean values are given in italic by type as discussed in the text, and a mean for all distances within parentheses

$[\text{CH}_3\text{Sn}(\text{OS}(\text{CH}_3)_2)_5](\text{ClO}_4)_3$, **1**

Bond distances/Å	Bond angles/°		
Sn1–O1	2.113(2)	O1–Sn1–O2	88.0(1)
Sn1–O2	2.099(2)	O1–Sn1–O3	94.7(1)
Sn1–O3	2.090(2)	O1–Sn1–O4	160.4(1)
Sn1–O4	2.098(2)	O1–Sn1–O5	78.9(1)
Sn1–O5	2.093(2)	O1–Sn1–C6	100.1(2)
Sn1–C6	2.113(2)	O2–Sn1–O3	169.1(1)
		O2–Sn1–O4	85.7(1)
		O2–Sn1–O5	88.4(1)
		O2–Sn1–C6	96.3(1)
		O3–Sn1–O4	88.3(1)
		O3–Sn1–O5	81.7(1)
		O3–Sn1–O6	93.7(1)
		O4–Sn1–O5	82.5(1)
		O4–Sn1–C6	98.9(1)
		O5–Sn1–C6	175.2(1)
Mean Sn–O/C value:		89.8/168.2	

Mean Sn–O/C value: 2.101

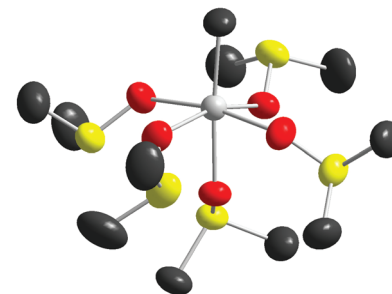


Fig. 1 Structure of the $[\text{CH}_3\text{Sn}(\text{OS}(\text{CH}_3)_2)_5]^{3+}$ unit in **1**, without a gap. Thermal ellipsoids (at 50% probability) are shown for all atoms; hydrogens have been removed for clarity.

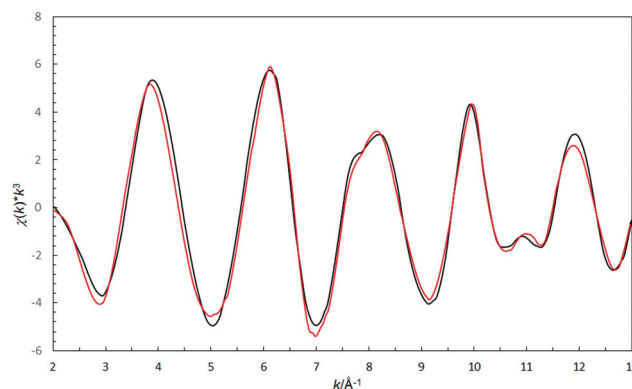


Fig. 2 The almost identical raw EXAFS spectra of solid **1** (red line) and a dmso solution of **1** (black line) show that the structure of the $[\text{CH}_3\text{Sn}(\text{OS}(\text{CH}_3)_2)_5]^{3+}$ unit in **1** is maintained in dmso solution.

graphic structure of **1**. It was not possible to separate the EXAFS scattering contribution of the Sn–O and Sn–C pathways, which are instead presented as an overall mean Sn–O/C bond distance of 2.097 Å, Table 2. The structure parameters are summarized in Table 3, and the fits of the EXAFS spectra in Fig. S3[†] and their Fourier transforms in Fig. S4[†].

Table 3 Mean bond distances, $d/\text{\AA}$, number of distances, N , Debye–Waller coefficients, $\sigma^2/\text{\AA}^2$, threshold energy, E_o , amplitude reduction factor, S_o^{-2} , and the goodness of fit from EXAFS studies of the **1** and its dmso solution at room temperature

Interaction	N	d	σ^2	E_o	S_o^{-2}	F
Solid $[\text{Sn}(\text{dmso})_5\text{CH}_3](\text{ClO}_4)_3$, 1						
Sn–O/C	6	2.097(1)	0.0047(1)	29 215.3(2)	0.90(1)	10.0
MS (SnO ₅ C)	3×6	4.21(1)	0.009(2)			
Sn···S	5	3.276(2)	0.0079(2)			
Sn–O–S	10	3.435(3)	0.0091(4)			
Sn···C	10	4.020(7)	0.012(1)			
dmso solution (mother liquid of 1)						
Sn–O/C	6	2.099(1)	0.0044(1)	29 216.1(2)	0.91(1)	8.9
MS (SnO ₅ C)	3×6	4.21(1)	0.009(2)			
Sn···S	5	3.284(2)	0.0084(2)			
Sn–O–S	10	3.448(3)	0.0092(3)			
Sn···C	10	4.015(7)	0.013(1)			

***N,N*-Dimethylthioformamide solvated tin(IV) ion**

Just as in the dmso solution, after more than a decade of storage, tin(II) reduces part of the dmtf molecules, in this case to (hydrogen)sulfide ions and dimethylamine, while itself is oxidized to tin(IV). The exact chemical reaction taking place and the required time are unknown. The crystals precipitating with time were not of sufficient quality for an accurate structure determination. However, the most electron-dense atoms, tin and sulfur, could be located. Two sulfur atoms, tentatively assigned as hydrogen sulfide ions, bridge the two tin(IV) ions and the octahedral coordination geometry around each tin(IV) ion is completed by four dmtf molecules, Fig. 3. Such a bonding arrangement is similar to patterns observed before for similar dmtf complexes,¹⁶ but also for similar structures involving tin(IV) and anionic S-donor ligands, Table S2.[†] Even though this structure could not be fully characterized, as the first tin(IV) structure with primarily neutral and exclusively monodentate S-donor ligands binding to tin(IV) it is definitely an interesting novel compound worth reporting. The basic structural information of 2 is listed in Table S3b[†] with the proposed position of the binuclear entity in the unit cell in Fig. S2.[†]

Comparison with other high-valent d¹⁰ metal ions

As stated in the Introduction, the use of both tin¹⁷ and lead¹⁸ ions is common in perovskite-based solar cells, and other

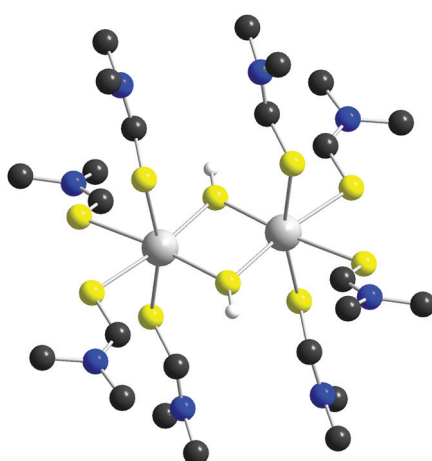


Fig. 3 Proposed structure of the $[\text{Sn}_2(\text{SH})_2(\text{SCHN}(\text{CH}_3)_2)_8]^{6+}$ entity in 2: dmtf hydrogens have been removed for clarity.

Table 4 Summary of the mean M–O bond distances for all reported six-coordinate gallium(III), indium(III), thallium(III), germanium(IV), tin(IV), and lead(IV) hydrates and solvates (hyd./sol.), and hydroxides (OH^-). The number of individual structure determinations are given in subscripted brackets, with a full description in the listed reference. The ionic radii, r_M^{n+} , have been calculated by subtracting $r_O = 1.34 \text{ \AA}$ from the mean M–O bond distance given by hydrates and solvates (top row), ref. 24. The Shannon radii, $r_M^{n+}_{\text{Sh.}}$, are listed for comparison, ref. 23

Mean M–O bond distance/ \AA							
M=	Ga^{3+}	In^{3+}	Tl^{3+}	Ge^{4+}	Sn^{4+}	Pb^{4+}	Ref.
hyd./sol.	1.957 ^[11]	2.130 ^[9]	2.229 ^[5]	n/a	n/a	n/a	Tables S4 and S5
OH^-	1.973 ^[7]	2.160 ^[2]	2.257 ^[1]	1.905 ^[5]	2.049 ^[20]	2.158 ^[4]	Tables S1, S4 and S5
r_M^{n+}	0.617	0.790	0.889	n/a	n/a	n/a	24
$r_M^{n+}_{\text{Sh.}}$	0.620	0.800	0.885	0.530	0.690	0.775	23

similar cells where their chemistry is advantageous. The other elements which exist as highly charged d¹⁰ ions, gallium(III),¹⁹ indium(III),²⁰ thallium(III),²¹ and germanium(IV),²² are also of interest within the broader terms of manufacturing semiconducting substrates, which makes a comparison between all of these chemical species valuable. Although the amount of structural data available is fairly limited, Tables S1, S4 and S5,[†] it is still enough to compare the calculated ionic radii for these ions in regard to those listed by Shannon,²³ Table 4.

The covalency between the tin(IV) ion and the methyl group makes any comparison between it and the remaining high-valent ions futile, as the charge reduction is significant which directly affects the resulting ionic radius of methyltin(IV). In fact, the effect of such a bond can be seen in a comparison of bond distances in monodentate Sn^{IV}O_6 , $\text{CH}_3\text{Sn}^{IV}\text{O}_5$, and $(\text{CH}_3)_2\text{Sn}^{IV}\text{O}_4$ cores, Table 5. The covalent bond between tin(IV) and the methyl group has a significant effect on the mean Sn–O bond distance, which increases on average by 0.060 \AA when one methyl group coordinates the tin(IV) ion and an additional 0.096 \AA when a second one is attached. It should be noted that methyltin(IV) represents approximately one fourth of all the six-coordinate compounds with an Sn–C bond.⁸

Conclusions

Tin(II) seems to be stable in aqueous solution over long periods of time, while in organic solvents, such as dmso and dmtf, the solvent is slowly reduced and tin(II) oxidized to tin(IV). In dmso, methyltin(IV) is formed, which just like dimethyltin(IV) generally feature octahedral coordination. The formation of a Sn–CH₃ bond greatly affects the mean Sn–O bond distances, when compared to those where tin(IV) ions only bind to O-donor ligands.

Here, the first solvate complex of methyltin(IV) has been reported and structurally characterized, $[\text{CH}_3\text{Sn}(\text{dmso})_5]^{3+}$. Conversely, in dmtf, the solvent is reduced to (hydro)sulfide ions and a $[\text{Sn}_2(\text{dmtf})_8(\text{SH})_2]^{6+}$ structural entity has been identified. These two solvate complexes add to the ever-expanding knowledge of solution-processing techniques used in the production of solar cells. Though this is a brief structural study and further experiments are required, the results presented herein could be a vital step in the development of a fairly straightforward wet chemical treatment of crystalline films.

Table 5 Comparison of Sn–O mean bond lengths based on the core bonding arrangement of monodentate six-coordinate tin(IV), including those with no Sn–C bond ($\text{Sn}^{\text{IV}}\text{O}_6$ core), one $\text{Sn}-\text{CH}_3$ bond ($\text{CH}_3\text{Sn}^{\text{IV}}\text{O}_5$ core) and two $\text{Sn}-\text{CH}_3$ bonds ($(\text{CH}_3)_2\text{Sn}^{\text{IV}}\text{O}_4$ core). No compounds with a $(\text{CH}_3)_n\text{Sn}^{\text{IV}}\text{O}_{6-n}$ core with $n > 2$ have been reported^a

Core _{CN6}	$d(\text{Sn}-\text{C})/\text{\AA}$	$d(\text{Sn}-\text{O})/\text{\AA}$	$d(\text{Sn}-\text{O/C})/\text{\AA}$	Ref.
$\text{Sn}^{\text{IV}}\text{O}_6$	n/a	2.052	2.052	Table S1
$(\text{CH}_3)\text{Sn}^{\text{IV}}\text{O}_5$	2.119	2.112	2.113	1, Table S6a
$(\text{CH}_3)_2\text{Sn}^{\text{IV}}\text{O}_4$	2.094	2.208	2.170	Table S6b

^a One compound with a $(\text{C}_6\text{H}_5)_3\text{Sn}^{\text{IV}}\text{O}_3$ core,²⁵ has been reported with mean $d(\text{Sn}-\text{C}) = 2.174 \text{ \AA}$ and $d(\text{Sn}-\text{O}) = 2.233 \text{ \AA}$, respectively.

Conflicts of interest

There are no conflicts to declare.

Acknowledgements

The authors are thankful for the structural suggestions from the crystallographic referee regarding the unanticipated compound 1. We gratefully acknowledge the Swedish Research Council for financial support. The use of the Stanford Synchrotron Radiation Lightsource, SLAC National Accelerator Laboratory, is supported by the U.S. Department of Energy, Office of Science, Office of Basic Energy Sciences under contract no. DE-AC02-76SF00515.

Notes and references

- 1 J. S. Manser, J. A. Christians and P. V. Kamat, *Chem. Rev.*, 2016, **116**, 12956–13008.
- 2 J. Ávila, C. Momblona, P. P. Boix, M. Sessolo and H. J. Bolink, *Joule*, 2017, **1**, 431–442.
- 3 I. Persson, P. D'Angelo and D. Lundberg, *Chem. – Eur. J.*, 2016, **22**, 18583–18592.
- 4 I. Persson, K. Lyczko, D. Lundberg, L. Eriksson and A. Płaczek, *Inorg. Chem.*, 2011, **50**, 1058–1072.
- 5 É. G. Bajnóczi, I. Pálinkó, T. Körtvélyesi, S. Bálint, I. Bakó, P. Sipos and I. Persson, *Dalton Trans.*, 2014, **43**, 17539–17543.
- 6 É. G. Bajnóczi, E. Czeglédi, E. Kuzmann, Z. Homonnay, S. Bálint, G. Dombi, P. Forgo, O. Berkesi, I. Pálinkó,
- 7 G. Peintler, P. Sipos and I. Persson, *Dalton Trans.*, 2014, **43**, 17971–17979.
- 8 F. H. Allen, *Acta Crystallogr., Sect. B: Struct. Sci.*, 2002, **58**, 380–388.
- 9 P. Portius, B. Peerless, M. Davis and R. Campbell, *Inorg. Chem.*, 2016, **55**, 8976–8984.
- 10 M. J. Hampden-Smith, T. A. Wark, A. Rheingold and J. C. Huffman, *Can. J. Chem.*, 1991, **69**, 121–129.
- 11 M. Veith and M. Reimers, *Chem. Ber.*, 1990, **123**, 1941–1944.
- 12 G. M. Sheldrick, *SHELX 2016/6: Program for Crystal Structure Refinement*, University of Göttingen, Göttingen, Germany, 2014.
- 13 G. N. George and I. J. Pickering, *EXAFSPAK — a Suite of Computer Programs for Analysis of X-ray Absorption Spectra*, Stanford Synchrotron Radiation Laboratory, Stanford, CA, USA, 2000.
- 14 A. Thompson, D. Attwood, E. Gullikson, M. Howells, K.-J. Kim, K. Kirz, J. Kortright, I. Lindau, Y. Liu, P. Pianetta, A. Robinson, J. Scofield, J. Underwood, G. Williams and H. Winick, *X-ray Data Booklet*, Lawrence Berkley National Laboratory, 2009.
- 15 S. I. Zabinsky, J. J. Rehr, A. Ankudinov, R. C. Albers and M. J. Eller, *Phys. Rev. B: Condens. Matter Mater. Phys.*, 1995, **52**, 2995–3009.
- 16 Ö. Topel, I. Persson, D. Lundberg and A.-S. Ullström, *Inorg. Chim. Acta*, 2011, **365**, 220–224.
- 17 J. A. Switzer, *J. Electrochem. Soc.*, 1986, **133**, 722–728.
- 18 A. Y. Shah, A. Wadawale, B. S. Naidu, V. Sudarsan, R. K. Vatsa, V. K. Jain, V. Dhayal, M. Nagar and R. Bohra, *Inorg. Chim. Acta*, 2010, **363**, 3680–3684.
- 19 M. M. Elsenety, A. Kaltzoglou, M. Antoniadou, I. Koutselas, A. G. Kontos and P. Falaras, *Polyhedron*, 2018, **150**, 83–91.
- 20 P. Srivastava and M. Kowshik, *Appl. Environ. Microbiol.*, 2017, **83**, e03091–e03016.
- 21 S. Khosroabadi and A. Kazemi, *Phys. E*, 2018, **104**, 116–123.
- 22 M. A. Mughal, R. Engelken and R. Sharma, *Sol. Energy*, 2015, **120**, 131–146.
- 23 R. D. Shannon, *Acta Crystallogr., Sect. A: Cryst. Phys., Diff., Theor. Gen. Crystallogr.*, 1976, **32**, 751–767.
- 24 J. K. Beattie, S. P. Best, B. W. Skelton and A. H. White, *J. Chem. Soc., Dalton Trans.*, 1981, 2105–2111.
- 25 N. C. Lloyd, B. K. Nicholson and A. L. Wilkins, *J. Organomet. Chem.*, 2006, **691**, 2757–2766.